Journal of Physics and Chemistry of Solids 90 (2016) 65–68

Contents lists available at ScienceDirect

Journal of Physics and Chemistry of Solids

journal homepage: www.elsevier.com/locate/jpcs

Current controlled negative differential resistance behavior in $Co_2FeO_2BO_3$ and $Fe_3O_2BO_3$ single crystals

E.C. dos Santos [a,1], D.C. Freitas [b], I. Fier [c], J.C. Fernandes [d], M.A. Continentino [b], A.J.A. de Oliveira [c], L. Walmsley [a,*]

[a] Departamento de Física, IGCE-Universidade Estadual Paulista – UNESP, C.P. 178, CEP 13500-970 Rio Claro, São Paulo, Brazil
[b] Centro Brasileiro de Pesquisas Físicas, Rua Xavier Sigaud 150, CEP 22290-180 Rio de Janeiro-RJ, Brazil
[c] Departamento de Física, Universidade Federal de São Carlos, C.P. 676, CEP 13560-970 São Carlos, São Paulo, Brazil
[d] Instituto de Física, Universidade Federal Fluminense, Campus da Praia Vermelha, CEP 24210-340 Niterói, Rio de Janeiro, Brazil

ARTICLE INFO

Article history:
Received 2 September 2015
Received in revised form
3 November 2015
Accepted 23 November 2015
Available online 1 December 2015

Keywords:
A. Ludwigites
D. NDR
D. Joule heating
D. Charge order depinning
D. Oscillations

ABSTRACT

I–V curves showing negative differential resistance (NDR) are reported for single crystals of $Co_2FeO_2BO_3$ at 315 K and 290 K and for $Fe_3O_2BO_3$ at 300 K, 260 K and 220 K. Resistivity measurements are presented for both systems, parallel and perpendicular to the *c* axis, in the range 315–120 K. The high hysteretic behavior of the *I–V* curves in $Co_2FeO_2BO_3$ around room temperature is discussed and the heat dissipated is estimated, suggesting an increase in the sample temperature of almost 22 K for the *I–V* curve at 315 K and a dominant contribution of Joule self-heating for the observed NDR. In contrast, insignificant hysteresis is observed on the *I–V* curves of $Fe_3O_2BO_3$ around room temperature. The depinning of charge order domains is suggested as the main contribution to the NDR phenomenon for $Fe_3O_2BO_3$. The high reproducibility of the NDR in the $Fe_3O_2BO_3$ single crystal allows its use as a low frequency oscillator, as it is demonstrated.

1. Introduction

The observation of current controlled negative differential resistance was reported in several systems for different ranges of temperatures, with Joule self- heating being the most accepted explanation of the NDR phenomenon. The increase of the current implies in a power increase in the sample and a consequent generation of heat. If the resistivity of the sample decreases when the temperature is increased, the heat drives the system from a high to a low resistivity state with the increase of the current and current controlled NDR is observed.

Alexandrov et al. [1] have developed a model to explain current controlled NDR in TiO_2 menristor. They used a thermal activation law for small polarons mobility and Ohm's law to write parametric equations for voltage and current as a function of power. Current controlled NDR was also observed in the Kondo insulator SmB_6 in the range 2–10 K [2]. The authors have also attributed the effect to Joule self-heating. However, they state that there is a nonlinear resistance in the current and voltage relationship. Nonlinear conduction was also observed in the current controlled *I–V* curves showing NDR in single crystals of the organic conductor $(TMET\text{-}TTP)_4PF_6$ in the approximate range 50–202 K by Mori et al. [3]. Using a phenomenological thermal approach, the authors found a very low value of specific heat when the experimental data was fitted, allowing them to conclude for the unimportance of Joule heating. Nonlinear conduction has also been found in the current controlled *I–V* curves in single crystals of $Pr_{0.63}Ca_{0.37}MnO_3$ observed in the charge order (CO) state that takes places below 240 K [4]. NDR was only observed below 170 K for the range of currents applied in the experiment. They have concluded that heating is not the cause of NDR but has some effect at high currents. In a similar way, Asamitsu et al. [5] have concluded that the changes in resistivity states in $Pr_{0.7}Ca_{0.3}MnO_3$ were not due to simple thermal effects.

Current controlled NDR curves observed around room temperature in single crystals of the oxy-borates $Co_2FeO_2BO_3$ and $Fe_3O_2BO_3$ are reported in this work. We aim to emphasize the differences observed in the NDR curves of these similar materials and their possible explanations. Both are compounds with the ludwigite $M_2MO_2BO_3$ chemical formula (M being a transition metal ion) and an orthorhombic *Pbam* structure. They are formed by substructures, which consist of three leg ladders (3LL) along the crystallographic *c* axis direction. These 3LL are composed by oxygen octahedra having transition metal ions at their centers. The projection of the whole structure in a plane perpendicular to the *c*

* Corresponding author.
E-mail address: walmsley@rc.unesp.br (L. Walmsley).
[1] Present address: Department of Physics, Norwegian University of Science and Technology, 7491, Trondheim, Norway.

http://dx.doi.org/10.1016/j.jpcs.2015.11.015
0022-3697/

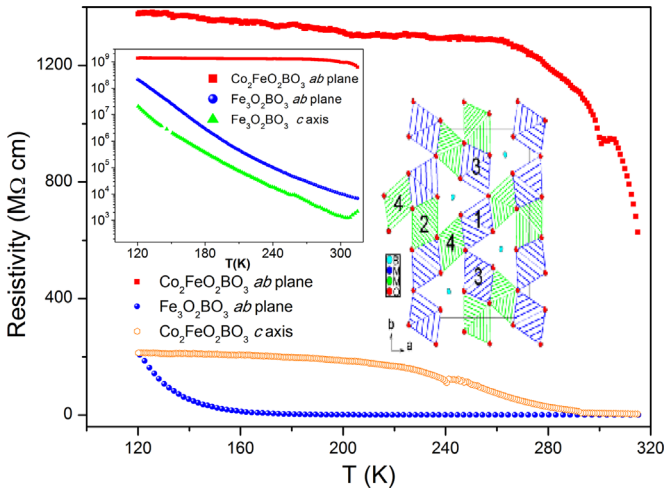

Fig. 1. Resistivity in the range 120–315 K; $Fe_3O_2BO_3$ perpendicular to the *c* axis (blue circles) and $Co_2FeO_2BO_3$ perpendicular (red squares) and parallel (open orange diamonds) to the *c* axis. Upper inset: In a log scale resistivities perpendicular to the *c* axis are shown, and for $Fe_3O_2BO_3$, resistivity parallel to the *c* axis (green triangles). Lower inset: Structure of $M_2MO_2BO_3$ in a plane perpendicular to the *c* axis. (For interpretation of the references to color in this figure legend, the reader is referred to the web version of this article.)

axis is shown in Fig. 1 (lower inset). The boron ions, in trigonal coordination, bind these substructures together. In $Co_2FeO_2BO_3$ the 4 and 2 sites are occupied by iron ions while cobalt ions occupy sites 1 and 3 [6–8]. In the case of $Fe_3O_2BO_3$, while the iron ions at sites 3 and 1 are divalent, those at sites 4 and 2 are almost trivalent and can be seen as formed by a background of Fe^{3+} ions with one extra electron for every three ions. The $Fe_3O_2BO_3$ is a unique system in the family of the ludwigites. X-ray diffraction measurements [9] have shown that this material has a structural transition at 283 K, which doubles the lattice period along the *c* axis, and has not been observed for any other member of this family. It occurs along the 4-2-4 three leg ladders, which extend along the *c*-axis. It consists of ions displacements in alternate directions, perpendicular to the *c* axis, in the central leg of the 4-2-4 ladders, which give rise to a dimerized phase. This charge ordered state has also been revealed by Mossbauer spectroscopy [10,11] with the transition identified to take place around 300 K. Due to its mainly one-dimensional character, this transition is accompanied by fluctuations and the appearance of short-range order, i.e., charge ordered domains, in an extended temperature interval around the critical temperature [9–12]. As the temperature decreases, the charge order becomes more robust. In the case of $Co_2FeO_2BO_3$, X-ray diffraction measurements could not find any charge order transition [7]. For both systems, magnetic order is found around 110 K [6–8].

2. Materials and methods

Single crystals of $Co_2FeO_2BO_3$ were grown as described in Ref. [7]. Those of $Fe_3O_2BO_3$ were synthesized as described in [6]. Both are single phases as confirmed by the X-ray spectra [6,7]. They grow as needles having the longest size parallel to the *c* axis. The samples, typical dimensions $Fe_3O_2BO_3$ ($0.5\ mm \times 0.2\ mm \times 0.2\ mm$) and $Co_2FeO_2BO_3$ ($1.0 \times 0.3 \times 0.3$) were carefully mounted on a sheet of mica attached to an aluminum sample holder. Gold wires (0.025 mm) were connected to the two silver conductive paint contacts in the opposite sides of the samples, perpendicular and parallel to the *c* axis. They were mounted inside a Janis CCS-150 closed cycle cryostat and the measurements were taken as the samples were cooled. Resistivity measurements have been performed applying constant current using a Keithley 2410 Source-meter for $Co_2FeO_2BO_3$ and a Keithley 2430 Source-meter for $Fe_3O_2BO_3$. In order to avoid leakage currents and to improve the accuracy, the guard mode option was used with the samples connected to a metallic guard ring. A very low current of 500 pA was applied to avoid reaching the voltage compliance of the meters. *I–V* curves have been recorded at each temperature, by applying current perpendicular to the *c* axis and measuring voltage with the same source-meters used to perform the resistivity measurements, starting from the higher temperatures. The perpendicular direction was chosen because for $Fe_3O_2BO_3$ better defined NDR curves around room temperature are obtained and oscillations are much easier observed in this direction.

3. Results and discussion

In Fig. 1, resistivity as function of temperature is shown for single crystals of $Co_2FeO_2BO_3$ perpendicular (red squares) and parallel (open orange diamonds) to the *c* axis. The resistivity of $Fe_3O_2BO_3$ perpendicular to the *c* axis is also displayed (blue circles). In the left inset perpendicular resistivities and the *c* axis resistivity of $Fe_3O_2BO_3$ (green triangles) are shown in a logarithmic scale. Around 304 K a broad minimum is seen in the *c* axis resistivity of $Fe_3O_2BO_3$ which could mark the charge order transition, as Mossbauer spectroscopy has found T_{CO} around 300 K. However, a definitive assignment was complicated by the fact that this minimum is thermal history dependent and was observed for some, but not all the measured samples. In polycrystalline Fe_2OBO_3, both Mossbauer spectroscopy and resistivity, could identify the charge order transition around the same temperature, in that case $T_C \sim 317$ K [13]. For $Co_2FeO_2BO_3$, features in the resistivity were clearly observed at some temperatures in both directions, marking differences in the temperature dependence. However, a charge order transition has not been detected by X-rays diffraction in this compound and it lacks information obtained by local techniques, thus, we could not make any attribution of those features in resistivity.

In Fig. 2, *I–V* curves showing NDR are displayed for $Co_2FeO_2BO_3$ at 315 K (blue circles) and 290 K (red squares). Both curves show hysteresis. The resistance at 290 K is larger than that at 315 K as can be taken from the *I–V* curve. The enclosed areas are the dissipated power, which can be obtained by integration. The times to take each curve were recorded and the amount of heat dissipated was 19.1 mJ and 24.8 mJ for the 290 K and 315 K *I–V* curves (positive current run), respectively. The specific heat is available for both samples up to 230 K for $Fe_3O_2BO_3$ and 275 K for $Co_2FeO_2BO_3$ [7] being $177.8\ J\ mol^{-1}\ K^{-1}$ and $137.6\ J\ mol^{-1}\ K^{-1}$ respectively. These values correspond respectively to 79% and 61% of the Dulong and Petit limiting value of the specific heat per mole around room temperature:

$$C = 3nR \tag{1}$$

R is the gas constant and n is the number of atoms per unit formula, in both cases here n=9. It is assumed that at 315 K the Dulong and Petit value of Eq. (1) corresponding to a value per mole of $225\ J\ K^{-1}$ has been reached at 315 K. In this case, the estimated heat capacity of the $Co_2FeO_2BO_3$ sample (1 mg) is $0.85\ mJ\ K^{-1}$ and the amount of heat of 24.8 mJ can be obtained with a final temperature T_f given by:

$$Q = 0.85\ mJK^{-1} \int_{315K}^{T_f} dT \tag{2}$$

Using the heat dissipated obtained previously, Eq. (2) gives a value of $T_f = 337$ K for the final temperature attained by the sample

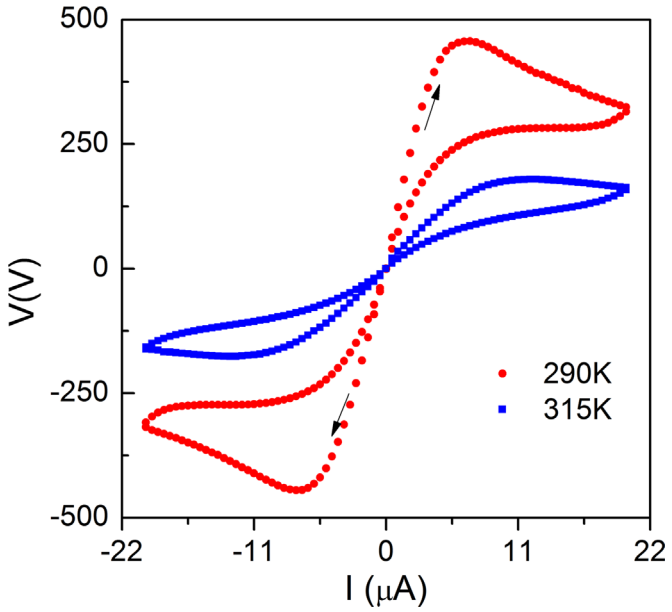

Fig. 2. *I–V* curves with the current applied perpendicular to the *c* axis at 290 K (red circles) and 315 K (blue squares) for single crystals of $Co_2FeO_2BO_3$ showing NDR and hysteresis. (For interpretation of the references to color in this figure legend, the reader is referred to the web version of this article.)

during the current positive cycle, showing a significant influence of heat. In this way, if it is considered that the resistivity of $Co_2FeO_2BO_3$ is activated in all range from 315 K to 337 K, Joule self-heating can be indeed the most important or maybe the only cause of NDR in $Co_2FeO_2BO_3$. However, this situation is not found on the *I–V* curves of $Fe_3O_2BO_3$.

In Fig. 3, *I–V* curves showing NDR are displayed for $Fe_3O_2BO_3$ at 300 K (red circles), 260 K (black squares) and 220 K (blue triangles), around and below the CO transition temperature as seen by Mossbauer [10,11]. Unlike *I–V* curves in $Co_2FeO_2BO_3$ that have shown hysteresis, for $Fe_3O_2BO_3$, hysteresis could hardly be

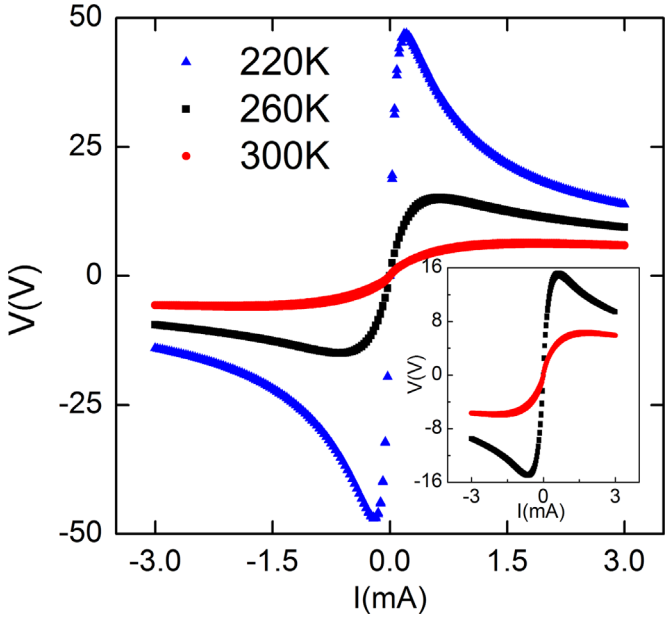

Fig. 3. *I–V* curves with the current applied perpendicular to the *c* axis at 220 K (blue triangles), 260 K (black squares) and 300 K (red circles) for single crystals of $Fe_3O_2BO_3$ showing NDR. Inset: details of the 260 K and 300 K curves showing discrete hysteresis. (For interpretation of the references to color in this figure legend, the reader is referred to the web version of this article.)

detected on the *I–V* curves (see inset of Fig. 3). Nevertheless, the specific heat of $Fe_3O_2BO_3$ tends to the same Dulong and Petit value at room temperature, the sample mass is even smaller than that of the $Co_2FeO_2BO_3$ single crystal and the resistivity is also activated in this same temperature range. These facts point to another dominant mechanism of NDR for $Fe_3O_2BO_3$ that takes place before any significant amount of heat has been dissipated.

In the search for such a mechanism, it is important to note the similarities of the $Fe_3O_2BO_3$ *I–V* curves and those observed for $Pr_{0.63}Ca_{0.37}MnO_3$ in Ref. [4]. Besides, both systems are mixed valence materials, in the case of $Fe_3O_2BO_3$, having Fe^{3+} and Fe^{2+} ions, and Mn^{4+} and Mn^{3+} in $Pr_{0.63}Ca_{0.37}MnO_3$. Both have charge ordered states. In both, the NDR phenomenon appears in the charge ordered state, is reproducible, and has small power dissipation. In Ref. [4], some possible mechanisms to explain NDR were suggested. First, the creation of conductive paths as the current increases, but in this case the reproducibility seen in the *I–V* curves seems unlikely. Second, that NDR is due to the depinning of the charge order domains above a threshold applied field. This possibility would help to understand why NDR is observed in the charge ordered state and disappears as a magnetic field of 8 T melts the charge order state into a ferromagnetic state. NDR has also been observed near 40 K in the prototypal charge-density wave (CDW) system $NbSe_3$ [14] above the threshold field for nonlinear conduction. Evidence of the significant contribution to the conductivity due to the depinning of these charge ordered domains emerge from those observations, reinforcing the possibility of observing NDR without significant Joule heating. The depinning of CDW systems was studied in linear chains compounds; see G. Grüner [15] for a review. In the specific case of $Fe_3O_2BO_3$, above a current threshold, which according to careful measurements performed for very low applied currents seems be around 0.3 μA, with a change of *I–V* behavior from linear to nonlinear, the CO collective state pinned by impurities becomes depinned and contributes to the total conductivity. The *I–V* curve reflects the two contributions, the single-particle linear contribution, and that of the depinned CO domains. The CO contribution to the conductivity increases with the increase of the current in a nonlinear way and overcomes the single-particle contribution for the conductivity for the range of currents NDR is observed.

Next, the application of a single crystal of $Fe_3O_2BO_3$ in an oscillator, as already known for systems that display NDR, like semiconductor devices, is described. The circuit used to drive low frequency oscillations in the sample is shown in Fig. 4a. Initially, we assume that the total current given to the circuit is larger than the current corresponding to the maximum voltage in Fig. 3. It splits in two components, one that charges the capacitor and other that passes through the sample. When the capacitor is charged all the current passes through the sample and, as it is driven to the NDR region, its potential decreases becoming smaller than the capacitor potential and promoting the discharge of the capacitor. Current can be driven again to the capacitor and a new charging cycle begins. The charging time depends on the current value and the total charge is given by the voltage (for a fixed capacitance). In Fig. 4b and c oscillations are shown applying current perpendicular to the *c* axis at 230 K and 300 K respectively. The oscillations can be driven at room temperature by a voltage of only 3 V.

4. Conclusions

In this work, we have presented *I–V* and resistivity data from two oxy-borates single crystals, $Co_2FeO_2BO_3$ and $Fe_3O_2BO_3$, which exhibit current controlled negative differential resistance phenomenon in the room temperature range. They have the same orthorhombic *Pbam* structure, similar values of room temperature

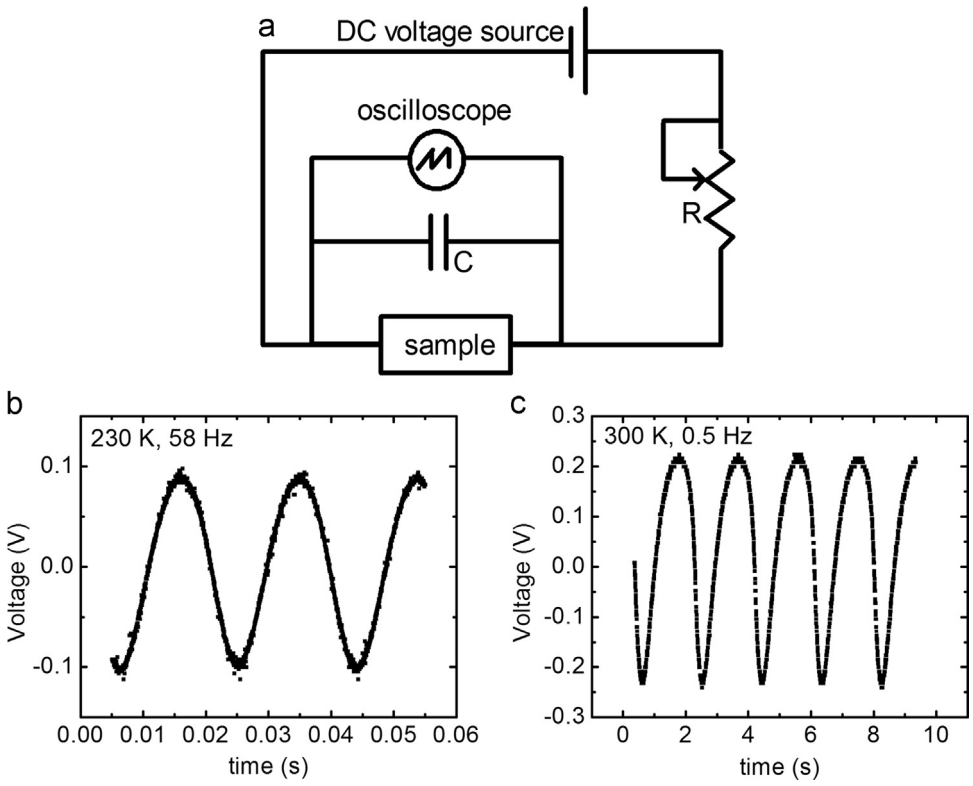

Fig. 4. (a) Circuit used to drive low frequency oscillations. Oscillations for the current in a direction perpendicular to the *c* axis, (b) at 230 K (58 Hz). (c) At 300 K (0.5 Hz).

specific heat and thermally activated resistivities around this temperature. In the case of $Co_2FeO_2BO_3$ a large hysteresis was observed on the *I–V* curves showing NDR. The amount of heat generated was quantified and Joule self-heating was identified as the main mechanism of NDR in $Co_2FeO_2BO_3$ single crystals. On the other hand, the lack of significant hysteresis on the *I–V* curves of $Fe_3O_2BO_3$ requires another mechanism for the observed NDR phenomenon besides Joule self-heating. The $Fe_3O_2BO_3$ system is the only system in the family of ludwigite oxy-borates that shows a structural transition associated with the formation of a transverse charge density wave. Consequently, it is natural to attribute the difference of the observed NDR phenomenon in $Fe_3O_2BO_3$ and $Co_2FeO_2BO_3$ to the existence of a CO in the former. Furthermore, the NDR behavior in this material is consistent with that observed in other charge ordered systems [4]. Then, the depinning of charge ordered domains is the dominant mechanism of NDR in $Fe_3O_2BO_3$ single crystals. It takes place before any significant amount of heat is dissipated, allowing very reproducible NDR curves to be obtained. This high reproducibility made possible the application of a $Fe_3O_2BO_3$ single crystal in a low frequency oscillator, which could be driven at room temperature by a voltage of only 3 V.

Acknowledgments

This work was partially supported by the Brazilian agencies Capes, FAPESP (2013/16266-0), FAPERJ (E-26/201.370/2014) and CNPq.

References

[1] A.S. Alexandrov, A.M. Bratkovsky, B. Bridle, S.E. Savel'ev, D.B. Strukov, R. Stanley Williams, Current-controlled negative differential resistance due to Joule heating in TiO_2, Appl. Phys. Lett. 99 (2011) 202104, http://dx.doi.org/10.1063/1.3660229.

[2] D.J. Kim, T. Grant, Z. Fisk, Limit cycle and anomalous capacitance in the Kondo insulator SmB_6, Phys. Rev. Lett. 109 (2012) 096601, http://dx.doi.org/10.1103/PhysRevLett.109.096601.

[3] T. Mori, T. Ozawa, Y. Bando, T. Kawamoto, S. Niizeki, H. Mori, I. Terasaki, Nonlinear dynamics of conduction electrons in organic conductors, Phys. Rev. B 79 (2009) (2009) 115108, http://dx.doi.org/10.1103/PhysRevB.79.115108.

[4] A. Guha, A.K. Raychaudhuri, A.R. Raju, C.N.R. Rao, Nonlinear conduction in $Pr_{0.63}Ca_{0.37}MnO_3$: effect of magnetic fields, Phys. Rev. B 62 (2000) 5320–5323.

[5] A. Asamitsu, Y. Tomioko, H. Kuwahara, Y. Tokura, Current switching of resistive states in magnetoresistive manganites, Nature 388 (1997) 50–52.

[6] R.B. Guimarães, M. Mir, J.C. Fernandes, M.A. Continentino, H.A. Borges, G. Cernicchiaro, M.B. Fontes, D.R.S. Candela, E. Baggio-Saitovitch, Cation-mediated interaction and weak ferromagnetism in $Fe_3O_2BO_3$, Phys. Rev. B 60 (1999) 6617–6622.

[7] D.C. Freitas, M.A. Continentino, R.B. Guimarães, J.C. Fernandes, E.P. Oliveira, R. E. Santelli, J. Ellena, G.G. Eslava, L. Ghivelder, Partial magnetic ordering and crystal structure of the ludwigites $Co_2FeO_2BO_3$ and $Ni_2FeO_2BO_3$, Phys. Rev. B 79 (2009) 134437, http://dx.doi.org/10.1103/PhysRevB.79.134437.

[8] N.B. Ivanova, N.Y. Kazak, Yu. V. Knyazev, D.A. Velikanov, L.N. Bezmaternykh, S. G. Ovchinnikov, A.D. Vasiliev, M.S. Platunov, J. Bartolomé, G.S. Patrin, Crystal Structure and Magnetic Anisotropy of Ludwigite $Co_2FeO_2BO_3$, J. Exp. Theor. Phys. 113 (2011) 1015–1024, http://dx.doi.org/10.1134/S1063776111140172.

[9] M. Mir, J.B. Guimarães, J.C. Fernandes, M.A. Continentino, A.C. Doriguetto, Y. P. Mascarenhas, J. Ellena, E.E. Castelhano, R.S. Freitas, L. Ghivelder, Structural Transition and Pair Formation in $Fe_3O_2BO_3$, Phys. Rev. Lett. 87 (2001) 147201, http://dx.doi.org/10.1103/PhysRevLett.87.147201.

[10] J.J. Larrea, D.R. Sánchez, F.J. Litterst, E.M. Baggio-Saitovitch, J.C. Fernandes, R. B. Guimarães, M.A. Continentino, Magnetism and charge ordering studied by ^{57}Fe Mössbauer spectroscopy, Phys. Rev. B 70 (2004) (2004) 174452, http://dx.doi.org/10.1103/PhysRevB.70.174452.

[11] A.P. Douvalis, A. Moukarika, T. Bakas, G. Kallias, V. Papaefthymiou, Mössbauer and magnetization studies of Fe_3BO_5, J. Phys. Cond. Matter 14 (2002) 3303–3320.

[12] P. Bordet, E. Suard, Magnetic structure and charge ordering in Fe_3BO_5: a single-crystal x-ray and neutron powder diffraction study, Phys. Rev. B 79 (2009) 144408, http://dx.doi.org/10.1103/PhysRevB.79.144408.

[13] J.P. Attfield, A.M.T. Bell, L.M. Rodriguez-Martinez, J.M. Greneche, R.J. Cernik, J. F. Clarke, D.A. Perkins, Electrostatic driven charge-ordering in Fe_2OBO_3, Nature 398 (1998) 655–658.

[14] R.P. Hall, M. Sherwin, A. Zettl, Negative differential resistance and instability in $NbSe_3$, Phys. Rev. Lett. 52 (1984) 2293–2296.

[15] G. Grüner, The dynamics of charge-density waves, Rev. Mod. Phys. 60 (1988) 1129–1181.